DOI: 10.4149/BLL_2017_065

Bratisl Med J 2017; 118 (6)
339 – 346

EXPERIMENTAL STUDY

MAPK pathway regulated the cardiomyocyte apoptosis in mice with post-infarction heart failure

Zhang Q[1,2], Lu L[2], Liang T[2], Liu M[2], Wang ZL[2], Zhang PY[3]

The First College of Clinical Medicine, Nanjing University of Chinese Medicine, Nanjing, Jiangsu Province, China. **zhangpeiyingxch@foxmail.com**

ABSTRACT

BACKGROUND: To explore the role of the MAPK signaling pathway in the cardiomyocyte apoptosis of mice with post-infarction heart failure (HF).

METHODS: Mice were divided into sham and myocardial infarction (MI) groups. Before surgery, the MI group was divided into SB203580 and PBS subgroups. A post-infarction HF model was established by ligating the left anterior descending coronary artery. Ventricular dilatation and cardiac function were observed by small animal echocardiography. The growth of primary cardiomyocytes was observed under an inverted phase contrast microscope. The mRNA and protein expressions of endoplasmic reticulum stress (ERS) markers, GRP78 and CHOP, were detected by qRT-PCR and immunofluorescence assay, respectively.

RESULTS: The MI group had enlarged left ventricle and decreased cardiac function. GRP78 and CHOP protein expressions in myocardial tissues, especially those of SB203580 subgroup, significantly increased ($p < 0.05$). The expressions of p-JNK and cleaved caspase 12 proteins, especially those of SB203580 subgroup, were significantly up-regulated. Cardiomyocytes of MI group were significantly more prone to apoptosis ($p < 0.05$), with SB203580 subgroup being more obvious.

CONCLUSION: MI was accompanied by ERS, probably involving the MAPK signaling pathway. SB203580, a specific inhibitor of this pathway, can relieve cardiomyocyte apoptosis and protect the myocardium by suppressing such stress *(Tab. 3, Fig. 7, Ref. 20)*. Text in PDF *www.elis.sk.*

KEY WORDS**:** myocardial infarction, heart failure, endoplasmic reticulum stress.

Introduction

After myocardial infarction (MI), cardiomyocytes undergo fibrosis and reduction in contractility, leading to heart failure (HF) and sudden cardiac death which are common destinies of many cardiac diseases (1). HF of MI patients suggests a decreased number of surviving cardiomyocytes, which causes deaths due to progressive aggravation (2). HF pathogenesis has mainly been attributed to hemodynamics changes, neuroendocrine activation and ventricular remodeling. Recently, with breakthroughs in the neuroendocrine field, researchers have found that cardiomyocytes undergo apoptosis and cannot be regenerated upon HF, thus absolutely reducing the number of functioning cells and myocardial contractility. This process is commonly accompanied by regulation of multiple signaling pathways, among which endoplasmic reticulum stress (ERS) has been widely studied (3–7).

The endoplasmic reticulum (ER) is an important organelle of cardiomyocytes in mammals. The metabolisms of membrane secretory proteins, glycosaminoglycans, cholesterol and calcium signaling proteins are directly related with the functions of ER. For example, secretory protein synthesis and folding as well as protein glycosylation and secretion - all take place in it. Dysfunction of ER may play a crucial role in myocardial ischemia-reperfusion injury (8–11). However, whether the MAPK signaling pathway is involved in the cardiomyocyte apoptosis of mice with post-infarction HF through ERS remains unclear hitherto.

Thereby motivated, we herein first established a post-infarction HF model of mice by ligating the left anterior descending coronary artery, aiming to explore ERS-mediated apoptotic pathway and its role in myocardial tissues. The pathogenesis of post-infarction HF was clarified, providing valuable evidence for treating and preventing this disease.

Materials and methods

Experimental animals

Twelve male SPF Kunming mice weighing 35–40 g were used, which were aged (3.1 ± 0.3) weeks on average. The mice were purchased from the institute of Laboratory Animal Science, Chinese Academy of Medical Sciences & Peking Union Medical College (China). All experimental procedures involving animal study were performed in accordance with the guidelines for Animal Ethical Committee (Xuzhou Central Hospital, China).

[1]The First College of Clinical Medicine, Nanjing University of Chinese Medicine, Nanjing, Jiangsu Province, China, [2]Xuzhou City Hospital of TCM, Xuzhou, Jiangsu Province, China, and [3]Department of Cardiology, Xuzhou Central Hospital, Xuzhou, Jiangsu Province, China

Address for correspondence: PY Zhang, Department of Cardiology, Xuzhou Central Hospital, The Liberation of South Road 199, Xuzhou 221009, Jiangsu Province, China.

Antibodies and reagents

GRP78 and α-actin antibodies, rabbit anti-mouse polyclonal CHOP antibody and goat anti-rabbit polyclonal secondary antibody were purchased from Santa Cruz (USA). Rabbit anti-mouse polyclonal JNK, p-JNK, caspase 12 and cleaved caspase 12 antibodies were bought from Cell Signaling Technology (USA). TUNEL assay kit was obtained from Roche (Germany).

Animal model establishment and experimental grouping (12)

The mice were divided into a Sham group (n = 4) and an MI group (n = 8). Before surgery, the MI group was divided into two subgroups that were treated by PBS (1 mg/g, n = 4) and SB203580 (1 mg/g, n = 4), respectively. A post-infarction HF model was established by ligating the left anterior descending coronary artery. For the sham group, the coronary artery was only passed through by silk thread but not ligated, and other operations were the same as those of the MI group. Standard limb and chest lead electrocardiograms were recorded before and after surgery. The modeling was successful if there were two or more ST segment elevations or arched ST segment elevations. After surgery, the mice were kept in cages, with regular light/dark cycles and free access to food and water. After successful modeling, echocardiographic indices of the two subgroups were recorded 2, 4 and 6 weeks after surgery, respectively.

Small animal echocardiography

Cardiac function changes in mice with post-infarction HF can be simply and conveniently detected by echocardiography, and the results are well correlated with indices measured by the hemodynamic method, such as maximal rate of rise in left ventricular pressure (dp/dtmax) and maximal rate of fall in left ventricular pressure (-dp/dtmin). Therefore, this method can accurately reflect the changes in left ventricular function. At the end of feeding, all surviving mice received echocardiography. The mice were anesthetized by intramuscular injection with Sumianxin (1–2 mL/kg), with the limbs and head fixed in the supine position, subsequently. The left ventricular images were collected horizontally at the papillary muscle of two-dimensional parasternal short-axis using an Acuson Sequoia 512 system at the probe frequency of 14 MHz. Meanwhile, the M-mode echocardiogram was obtained under two-dimensional guidance, with over 10 cardiac cycles recorded. The echocardiogram was used to measure left ventricular end-diastolic diameter (LVEDD), left ventricular end-systolic diameter (LVESD), left ventricular systolic anterior wall thickness (Aws), left ventricular diastolic anterior wall thickness (Awd), left ventricular systolic posterior wall thickness (Pws), left ventricular diastolic posterior wall thickness (Pwd), heart rate (HR) and ejection fraction (EF). Left ventricular fractional shortening (FS) was calculated according to FS% = [(LVEDD-LVESD)/LVEDD] × 100%.

Detection indices

After the mice had been sacrificed by cervical dislocation, the heart was taken and dried with filter paper. The left ventricle (LVW) (including the interventricular septum) and the right ventricle (RVW) (excluding the interventricular septum) were weighed, respectively, and the ratios of LVW/body weight (LVW/BW) and RVW/BW were calculated, representing the left ventricular hypertrophy index and the right ventricular hypertrophy index, respectively. The myocardium of non-infarcted left ventricular region was cut into several blocks and stored immediately in a –70 °C refrigerator. Then the lung tissue was weighed, and the lung weight/BW (LUNGW/BW) ratio was calculated.

Myocardial pathomorphology

The myocardium of infarcted left ventricular region was taken, rinsed with PBS at 4 °C and fixed with 4 % paraformaldehyde solution. Forty-eight hours later, the tissue was routinely dehydrated, paraffin-embedded, cut into 4 μm-thick sections, HE-stained and observed under a light microscope.

Western blotting

Myocardial tissues (30 mg) were homogenized, lysed, ultrasonicated and centrifuged at high speed. Then the supernatant was collected to measure the protein concentration on a Bio-Rad spectrophotometer using the Coomassie brilliant blue method, and stored at –20 °C after subpackaging. Protein solution containing 50 μg protein sample was subjected to 10 % sodium dodecyl sulfonate-polyacrylamide gel electrophoresis (SDS-PAGE). Then the protein was transferred onto a nitrocellulose membrane by the semi-dry method. Afterwards, the membrane was blocked for 4 h at room temperature (blocking solution: TBST solution containing 5 % skimmed milk), washed and incubated overnight with primary GRP78 antibody (1:400 dilution), primary CHOP antibody (1:800 dilution), primary caspase 12 antibody (1:1000 dilution), primary JNK antibody (1:1000 dilution) and primary p-JNK antibody (1:1000 dilution), respectively at 4 °C. After washing, the membrane was incubated with appropriate secondary antibodies at room temperature for 1 h, color-developed with the chemiluminescence method and exposed to X-ray. To avoid the influence of loading protein amounts, the Western blotting results were corrected by α-actin. The integral absorbances (IAs) of protein bands were analyzed by Image-ProPlus. IA = Average absorbance ×

Tab. 1. LVW/BW, RVW/BW and LUNGW/BW 2, 4 and 6 weeks after surgery.

	Group	2 w	4 w	6 w
LVW/BW (mg/g)	Sham (n=4)	1.57±0.20	1.56±0.43	1.55±0.52
	PBS (n=4)	1.61±0.12	1.68±0.44	1.77±0.12
	SB203580 (n=4)	1.72±0.14	1.78±0.51	1.81±0.52
	F value	5.27	3.82	1.28
	P value	0.017	0.025	0.044
RVW/BW (mg/g)	Sham	0.56±0.18	0.58±0.28	0.58±0.27
	PBS	0.59±0.21	0.61±0.19	0.70±0.22
	SB203580	0.66±0.21	0.72±0.24	0.78±0.43
	F value	4.38	5.48	4.38
	P value	0.021	0.016	0.025
LUNGW/BW (mg/g)	Sham	2.40±0.18	2.41±0.19	2.53±0.29
	PBS	3.26±0.17	3.82±0.11	4.03±0.21
	SB203580	3.55±0.39	4.12±0.44	5.52±0.43
	F value	4.39	5.58	7.38
	P value	0.024	0.017	0.018

Tab. 2. Echocardiographic indices.

Group	LVEDD			LVESD			Aws			Awd			Pws			Pwd			FS%			HR			EF (%)		
	2 w	4 w	6 w	2 w	4 w	6 w	2 w	4 w	6 w	2 w	4 w	6 w	2 w	4 w	6 w	2 w	4 w	6 w	2 w	4 w	6 w	2 w	4 w	6 w	2 w	4 w	6 w
Sham (n=4)	1.97±0.17	1.98±0.13	1.99±0.11	3.23±0.13	3.33±0.12	3.35±0.18	1.40±0.08	1.41±0.10	1.40±0.11	0.76±0.05	0.75±0.18	0.76±0.12	1.35±0.18	1.33±0.24	1.34±0.11	0.85±0.15	0.88±0.17	0.86±0.18	49.12±2.23	49.38±2.19	50.29±2.13	336±148	342±128	337±182	87.51±5.26	88.32±3.42	87.28±2.34
PBS (n=4)	3.79±0.16	4.29±0.19	4.47±0.21	5.46±0.12	5.92±0.10	6.24±0.16	0.96±0.07	0.82±0.10	0.80±0.14	0.87±0.09	0.75±0.05	0.76±0.05	1.32±0.22	1.71±0.15	1.50±0.20	0.82±0.10	0.92±0.05	0.84±0.06	32.50±4.91	21.14±1.34	18.42±1.51	406±147	430±168	458±212	78.36±4.36	69.12±3.65	63.3±1.92
SB203580 (n=4)	4.17±0.18	4.83±0.32	4.94±0.33	5.81±0.13	6.69±0.38	7.11±0.22	0.88±0.04	0.76±0.03	0.68±0.04	0.92±0.08	0.76±0.02	0.66±0.02	1.34±0.13	1.66±0.13	1.42±0.33	0.83±0.21	0.90±0.03	0.82±0.03	33.47±4.48	20.33±2.18	14.33±0.21	407±212	439±125	498±112	82.3±3.33	55.3±2.98	45.4±3.23

area, where the ratio of $IA_{target\ protein}/IA_{\alpha\text{-actin}}$ represents the relative expression level of target protein.

Detection of cardiomyocyte apoptosis

Myocardial tissues in the middle of the left ventricular anterior wall were collected to prepare paraffin sections. *In situ* detection of myocardial apoptosis in tissue sections was conducted according to kit's instructions using the TUNEL assay. Under the light microscope, normal myocardial cells were stained bluish green, and apoptotic nuclei were irregularly stained brown. Ten high-power visual fields were selected randomly from each section in the area where apoptotic cells were distributed. Then the number of apoptotic cells per 100 cells was calculated, with percentage (%) representing the apoptotic index (AI).

Culture and identification of cardiomyocytes

The mice were soaked in 75 % ethanol for a few seconds, and the following steps were performed on super-clean bench. Neonatal mice were sacrificed by cervical dislocation, with their head and limbs fixed in the supine position. The thorax was cut open from the axilla by an ophthalmic scissor, from which the heart was scissored off and quickly placed into pre-cooled PBS solution to wash away residual red blood cells. The atrium was scissored off, and ventricular muscle tissue was taken and put into another dish, cut into pieces (about 1 mm × 1 mm × 1 mm) and added with type II collagenase of 5 times the volume of the tissue. The resulting suspension was transferred to a vial of penicillin, digested for 4 min through repeated pipetting, and left still. After the supernatant had been discarded, an appropriate amount of type II collagenase was added, and the mixture was repeatedly pipetted and naturally precipitated to collect the supernatant. The above steps were repeated 4–5 times until the tissue mass was completely digested. The supernatant obtained each time was transferred to a centrifuge tube, added with an equal volume of DMEM containing 15 % fetal bovine serum (FBS) to terminate the action of collagenase, and centrifuged at 800 r/min for 10 min to discard the supernatant. The cell precipitates were collected and mixed in DMEM (containing 15 % FBS, 105 U/L penicillin and 105 U/L streptomycin, pH 7.2) to prepare a cell suspension. The differential adherence method was used to isolate and purify myocardial cells. The cell suspension was inoculated into culture flasks and cultured in a 5 % CO_2 incubator at 37 °C for 2 h. Non-myocardial cells adhered to the flask bottom faster, whereas myocardial cells remained in the suspension state. The cell suspension was sucked out and added with 5-Brdu to 0.1 mmol/L to inhibit the proliferation of non-myocardial cells. The cell suspension was inoculated into 6-well plates at a density of about 1×10^6 cells/cm^3, and cultured in a 95 % O_2 + 5 % CO_2 incubator at 37 °C. The culture medium was changed

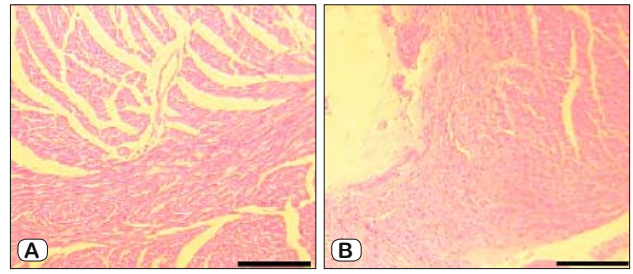

Fig. 1. HE staining results of (A) Sham group and (B) MI group. Magnification: 200x.

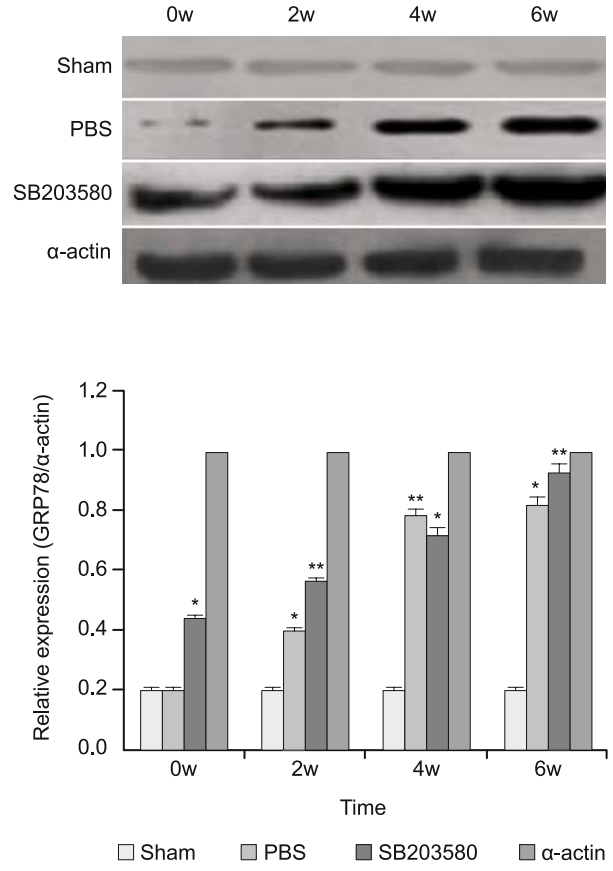

Fig. 2. GRP78 protein expressions in different groups 2, 4 and 6 weeks after surgery. Compared with the Sham group, * p < 0.05, ** p < 0.01.

48 h later. The solution was changed once every 2 to 3 days. The myocardial cells were thereafter cultured in DMEM containing 15 % FBS for 3 to 4 days. Intervention was given when the adherent myocardial cells extended pseudopodia and connected into pieces while beating well and tending to be synchronized. By using the immunofluorescence method, myocardial cells were identified by detecting cytoplasmic α-actin with rabbit anti-mouse primary actin antibody and FITC goat anti-rabbit secondary antibody.

Detection of GRP78 and CHOP protein expressions by immunofluorescence assay

The myocardial cells of neonatal mice underwent primary culture. Non-myocardial cells were first removed by the differential adherence method, and then viable cells were counted by trypan blue staining. The myocardial cells were adjusted to 5×10^8 cells/L with 20 % bovine serum medium and inoculated into 12-well plates (a polylysine-treated coverslip was placed in each well for cell growth), 1.5 mL per well. Twenty-four hours after treatment, the cells were washed with PBS three times. Subsequently, the coverslips were taken out, fixed with 4 % paraformaldehyde for 30 min, washed with PBS 3 times, incubated in 4 % methanol containing 0.1 % TritonX-100 for 20 min, blocked with 10 % normal goat serum for 30 min at room temperature, incubated overnight with rabbit anti-mouse primary polyclonal GRP78 and CHOP antibodies, respectively at 4 °C, washed with PBS three times again, incubated with 1:50 FITC-labeled goat anti-rabbit IgG antibody at room temperature for 1 h, washed with PBS 3 times, and finally mounted with 90 % glycerol. The test samples were placed under a laser scanning confocal microscope, and the excitation wavelength of HeNe laser was determined to be 543 nm by HQ590-70 emission filter through 10-fold and 100-fold objective lens (eyepiece: 10×), respectively. The cell scanning parameters were optimized

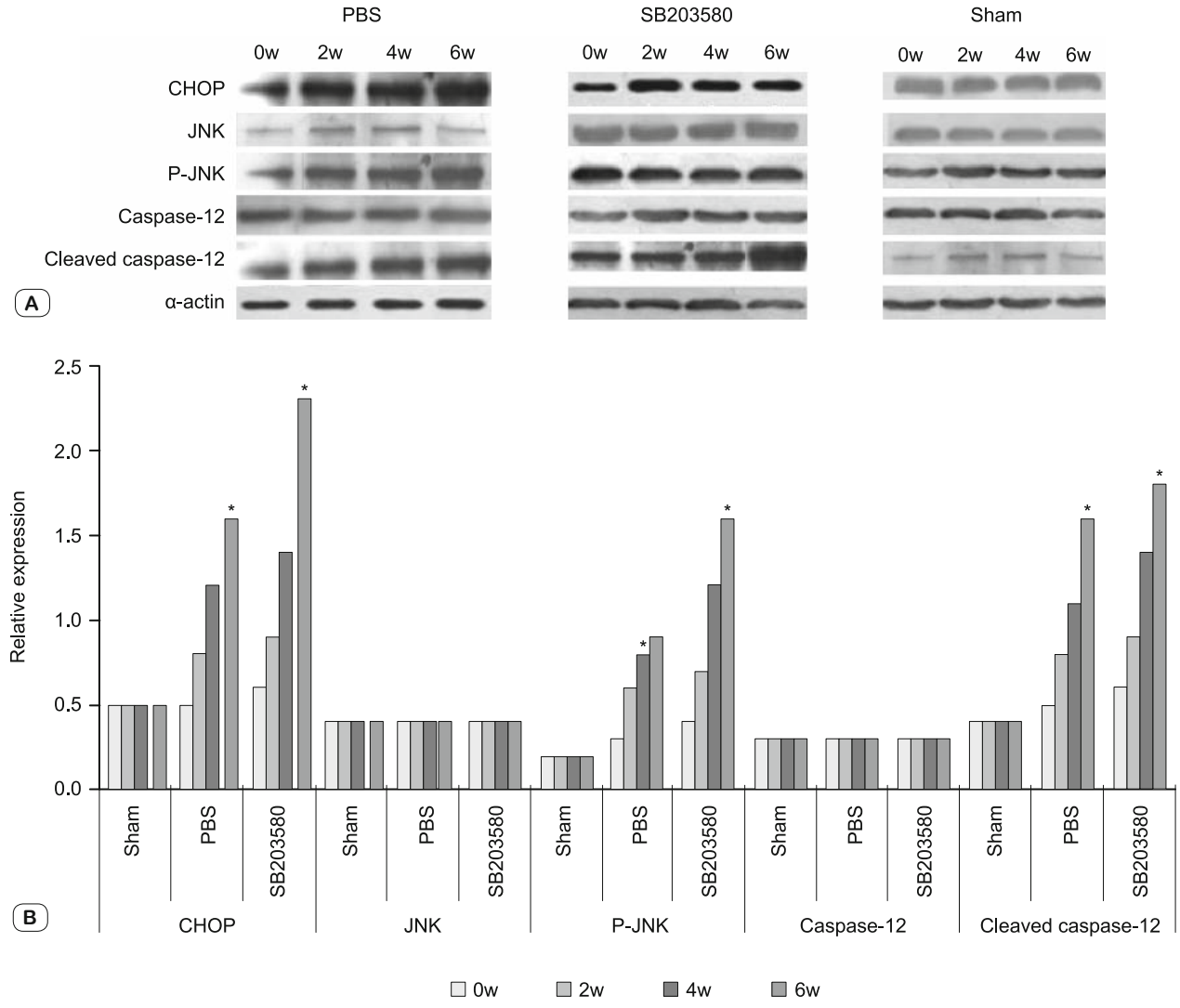

Fig. 3. Cardiomyocyte apoptosis under ERS was mediated by CHOP, JNK and caspase 12 pathways. A: Western blot results of different groups 2, 4 and 6 weeks after surgery; B: statistical analysis results. Compared with the Sham group, * $p < 0.05$.

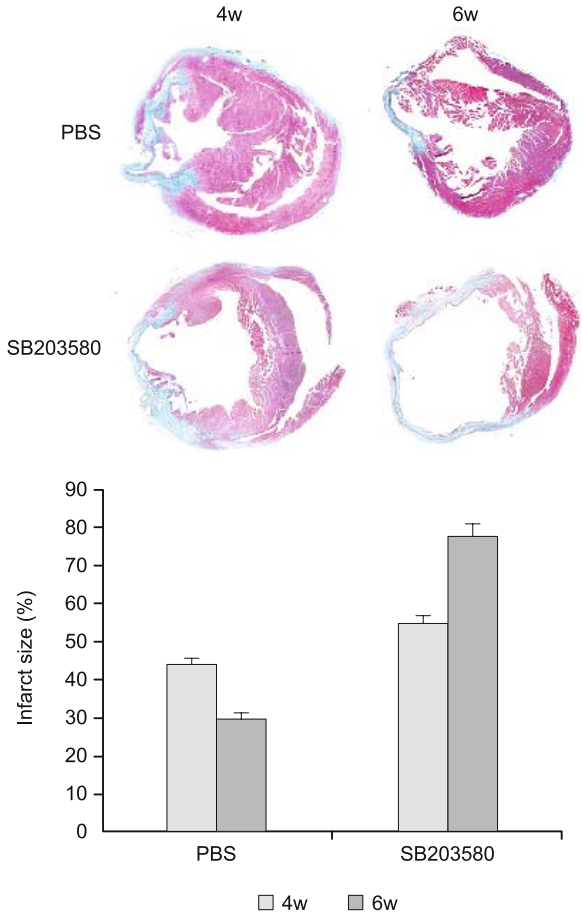

Fig. 4. MI areas. A: Masson staining results. Magnification: 100x; B: statistical analysis results.

after pre-scanning using LaserSharp2000 program (Bio-Rad, CA, USA), by which cell photographs were scanned and stored. Data measurements were carried out by Lasersharp2000.

Real-time quantitative PCR (qRT-PCR)

Total RNA was extracted by UNIQ-10 column extraction kit (Shanghai Sangon Biotech Co., Ltd., China). RNA (2 μL) was quantified. An equal amount of RNA from each group was taken, with the total volume adjusted to 10 μL with RNase free water. After addition of other reagents, cDNA was synthesized by reverse transcription in a reaction system with the total volume of 20 μL. PCR amplification was conducted by using 2 μL of cDNA in a 20 μL reaction system. GRP78 primer, upstream: 5'-CTGGGTACATTTGATCTGACTGG-3', downstream: 5'-GCATCCTGGTGGCTTTCCAGCCATTC-3', total length: 345 bp; CHOP primer, upstream: 5'-AGCAGAGGTCACAAGCACCT-3', downstream primer: 5'-CTGCTCCTTCTCCTTCATGC-3', total length: 166 bp; β-actin primer, upstream: 5'-CTACAATGAGCTGCGTGTGGC-3', downstream: 5'-CAGGTCCAGACGCAGGATGGC-3', total length: 270 bp. PCR conditions were as follows: pre-denaturation at 95 °C for 30 s, denaturation at 95 °C for 5 s and annealing at 60 °C for 31 s, 40 cycles in total. The relative concentrations were calculated for inter-group comparisons.

Masson staining

Paraffin sections were deparaffinized, rehydrated, and washed with tap water and distilled water successively. Cell nuclei were stained with Regaud's or Weigert's hematoxylin solution for 5–10 min, thoroughly rinsed with water (hydrochloric acid-ethanol medium was used for differentiation in case of overstaining), and thereafter washed with distilled water. Myocardial tissues were stained with Masson ponceau-acid fuchsin solution for 5–10 min, immersed and washed in 2 % aqueous acetic acid solution for a moment, differentiated with 1 % aqueous solution of phosphomolybdic acid for 3–5 min, directly stained with aniline blue or light green solution for 5 min, immersed and washed again in 0.2 % acetic acid aqueous solution for a moment, and subjected to gradient dehydration with 95 % ethanol and absolute ethanol, xylene transparentization and neutral gum mounting. The collagen fiber, mucus and cartilage were stained blue (or green if light green solution was used). The cytoplasm, muscle, cellulose and neuroglia were stained red, and the nucleus was stained darkish blue.

Statistical analysis

All experimental data were analyzed by SPSS13.0 and expressed as mean ± standard deviation (x ± s). Differences among multiple groups were compared by one-way analysis of variance.

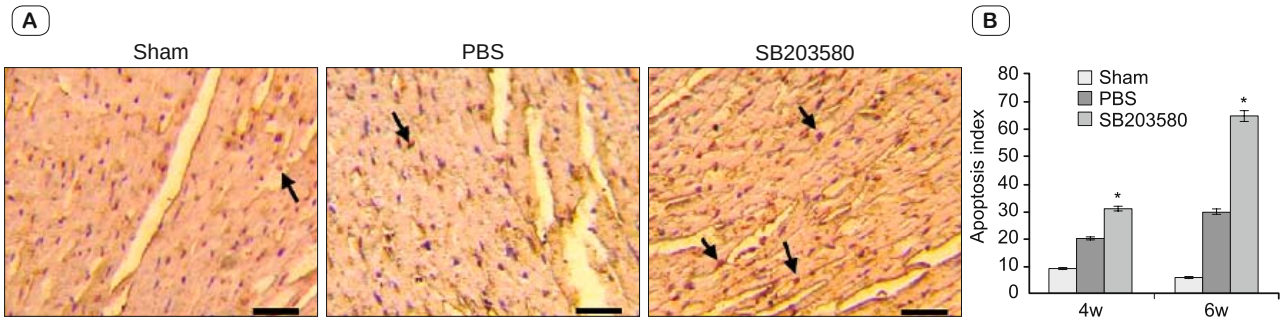

Fig. 5. Apoptosis of cardiomyocytes from post-infarction HF mice. A: TUNEL staining results. Magnification: 100x.The nuclei of apoptotic cells were stained brown in different degrees; B: statistical analysis results. Compared with the Sham group, * $p < 0.05$.

Results

General information after modeling

Compared with the Sham group, the MI group had whitened heart surface in the dominant area, weakened local myocardial motion and expanded left atrial appendage after ligation of the coronary artery. After the chest had been closed, standard limb and chest lead electrocardiograms showed two and above ST segment elevations or arched ST segment elevations. Two weeks after surgery, the MI group had already suffered from accelerated breathing, anorexia and reduced activity. The myocardial tissues from the anterior ventricular wall of the MI group were greyish white in color, but those of the Sham group hardly changed. Compared with the Sham group, the MI group, especially the SB203580 subgroup, had significantly increased LUNGW/BW two weeks after surgery (Tab. 1). Therefore, SB203580 aggravated HF and pneumonedema. The HE staining results of myocardial tissues are presented in Figure 1.

Echocardiographic indices

Compared with the Sham group, echocardiography displayed that the PBS subgroup began to have elevated LVEDD and LVESD two weeks after surgery. At this time, Awd, EF and FS% were decreased and kept decreasing further thereafter. HR changed oppositely. The indices were poorer after SB203580 treatment (Tab. 2). Thus, the MI model had been successfully established.

GRP78 protein expression was up-regulated in cardiomyocytes from post-infarction HF mice

Compared with the Sham group, GRP78 expression in the PBS subgroup was up-regulated by 133 %, 173 % and 198 %, respectively 2, 4 and 6 weeks after surgery, and that in the SB203580 subgroup was up-regulated by 155 %, 184 % and 233 %, respectively at the same time points. There were statistically significant differences ($p < 0.05$) (Fig. 2).

Cardiomyocyte apoptosis under ERS was mediated by CHOP, JNK and caspase 12 pathways

Compared with the Sham group, the expression levels of CHOP, p-JNK and cleaved caspase 12 in the MI group, especially those of the SB203580 subgroup, were both significantly up-regulated ($p < 0.05$). However, the levels of JNK and caspase 12 proteins were similar ($p > 0.05$) (Fig. 3).

MI areas

Masson staining showed that the SB203580 subgroup had significantly larger MI areas than the PBS subgroup 4 and 6 weeks after surgery ($p < 0.05$) (Fig. 4).

Apoptosis of cardiomyocytes from post-infarction HF mice

The TUNEL assay showed that AI of the Sham group was 3.15 ± 0.72 % and those of the MI group were 19.47 ± 0.99 %, 28.92 ± 1.36 % and 40.43 ± 1.21 %, respectively 2, 4 and 6 weeks after surgery (Fig. 5).

Flow cytometry exhibited that cardiomyocytes of the MI group were significantly more prone to apoptosis 6 weeks after surgery than those of the Sham group ($p < 0.05$), with the SB203580 subgroup being more obvious ($p < 0.05$) (Fig. 6).

GRP78 and CHOP protein expression levels detected by immunofluorescence assay

The immunofluorescence assay also showed that GRP78 and CHOP protein expression levels in the MI group were significantly higher than those of the Sham group ($p < 0.05$) (Fig. 7). The GRP78 and CHOP mRNA expression levels followed the same trend (Tab. 3).

Discussion

As a heart disease commonly occurring in clinical practice, MI is mainly caused by insufficient blood supply of local tissues of the heart due to coronary artery obstruction. Myocardial ischemia and hypoxia may induce a decline in myocardial contractility, leading to HF and myocardial fibrosis. The onset of post-infarction HF has been closely related to inflammatory reaction. Among multiple mechanisms, the role of ERS has gradually attracted attention.

ER plays an important role in polypeptide synthesis and post-translational modification of polypeptides into intracellular or secretory proteins. ERS may occur when ER is unbalanced for some reason, producing excessive misfolded proteins (6). ERS

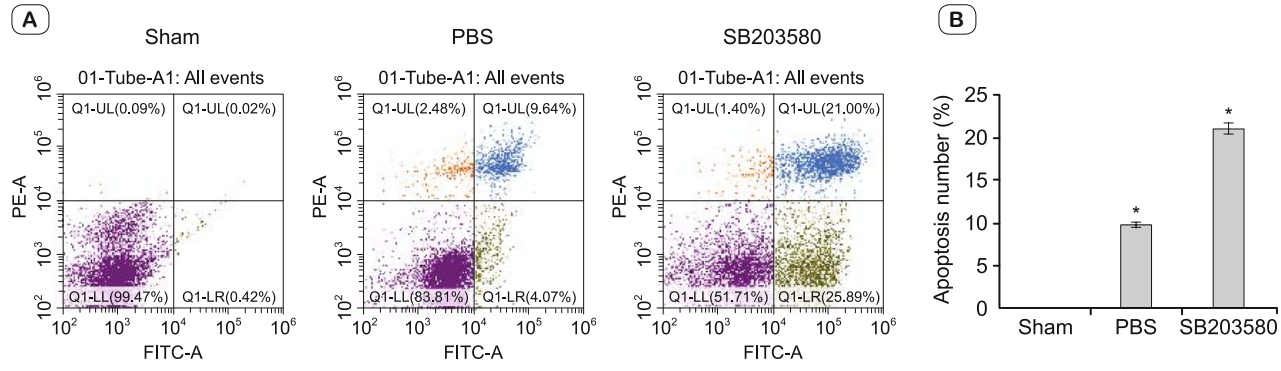

Fig. 6. Apoptosis of cardiomyocytes from post-infarction HF mice. A: Flow cytometry results; B: statistical analysis results. Compared with the Sham group, * $p < 0.05$.

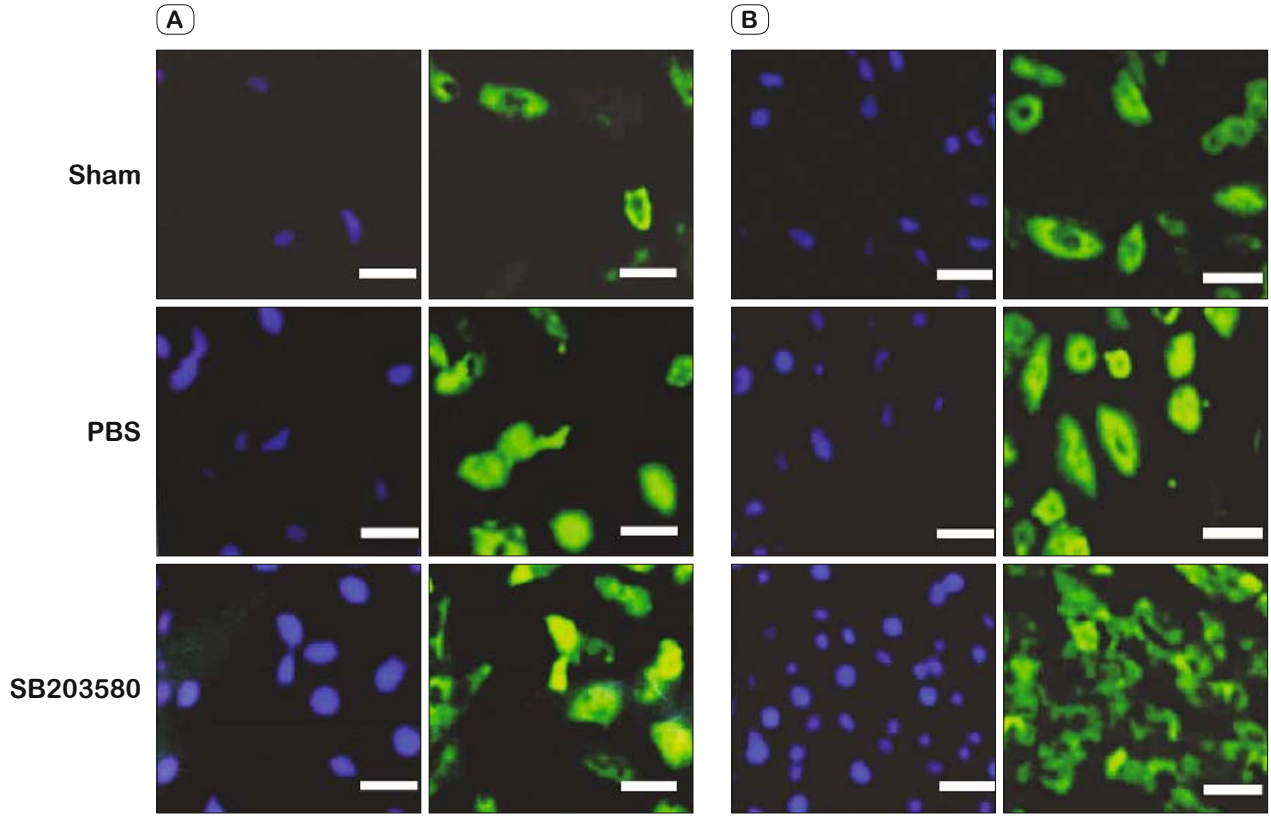

Fig. 7. Immunofluorescence assay results for (A) GRP78 protein and (B) CHOP protein expressions in cardiomyocytes. Compared with the Sham group, * p <0.05.

is a self-protective mechanism of cells to restore homeostasis, but too strong or prolonged stress response can lead to apoptosis.

ERS usually has a common molecular basis. GRP78 is one of the proteins playing dominant roles in ERS, as well as a member of the HSP70 protein family. Similar to other HSP70 family proteins, GRP78 is a protein-like substance with ATP adenosine triphosphatase activity. This protein contains two highly conservative domains, i.e. an about 44,000 ATPase domain at the N-terminus and a binding domain that is located at the C-terminus and can bind proteins to be folded. GRP78 can recognize and bind seven hydrophobic amino acid residues in the unfolded region, and promote protein folding through conformational changes in the ATPase binding domain. With the help of several HSP40 family protein homologues, GRP78 can further function in ER. These protein members usually have highly conservative J-domains at the N-terminus, which can interact with GRP78 to activate the ATPase activity, and the C-terminus can bind proteins to be folded (5). Therefore, GRP78, as an ER molecular chaperone, can sensitively respond to the activation of such stress (6). In our study, GRP78 protein was expressed continuously in the myocardial cells of HF mice after MI, and the expression level was constantly increased along with aggravation of HF. Therefore, in the mouse model of post-infarction HF, GRP78 may be accompanied by the activation of ERS response. Researchers have found such activation upon myocardial ischemia and atherosclerosis (7, 8). The common mechanism is based on damaged ER homeostasis owing to overload caused by the lack of nutrients, calcium overload, lipid overload, viral infection, drugs, toxins and increased synthesis of secretory proteins, further activating the stress response (9). It is generally believed that the signal pathways of ERS-induced apoptosis are CHOP, JNK and caspase 12.

Tab. 3. GRP78 and CHOP mRNA expression levels 6 weeks after surgery.

Group	GRP78 mRNA	CHOP mRNA
Sham	1	1
PBS	2.10±0.08*	2.42±0.05*
SB203580	2.68±0.07*#	2.91±0.03*#

*Comparison between Sham group and PBS subgroup, $p < 0.05$; #Comparison between PBS and SB203580 subgroups, $p < 0.05$.

The above apoptotic pathways are different from the classic ones of death receptors. When ER is overloaded and the stress compensation fails to work under pathological conditions such as accumulation of toxic substances and calcium overload, apoptosis can be mediated via the above three pathways, thereby protecting the survival of vital organs. ERS-mediated apoptotic pathways exist in various systems of human body, such as heart, kidney, brain and tumors (10–13).

Cominacini et al. reported that the expression levels of 593 kinds of proteins significantly changed upon HF, of which the proteins related to ERS response, apoptosis and cytoskeletal re-

modeling played key roles (14). Wei et al. found that in a rat model of HF caused by aortic coarctation-induced stress overload, ERS remained after modeling, and promoted myocardial cell apoptosis, mainly due to the reaction after activation of the CHOP pathway (15). In this study, after the MAPK signaling pathway had been inhibited by SB203580, the myocardial cell apoptosis was promoted significantly, and the expression level of ERS-related signaling pathway protein GRP78 was further increased. Therefore, after the MAPK signaling pathway had been suppressed, ERS was compensatorily facilitated during post-infarction heart repair, and the apoptosis of myocardial cells was promoted, in which caspase 12 played crucial roles (16). Caspase 12 is a specific mediator of ERS-induced reactive apoptosis localized on the ER surface, irrelevant to the apoptotic pathways not involving ER. In addition, the activation of caspase 12 can enable ERS to independently induce apoptosis (17), suggesting that the roles of JNK, caspase 12 and CHOP in ERS-induced reactive apoptosis are different in various HF models (18–20). In our study, the expression levels of CHOP, p-JNK and cleaved caspase 12 proteins, which were all up-regulated in model rats, were elevated as HF was aggravated, accompanied by significantly increased AI. Hence, CHOP, JNK, and caspase 12 were involved in cardiomyocyte apoptosis during post-infarction HF. After the activity of the MAPK signaling pathway had been inhibited by SB203580, cardiomyocyte apoptosis induced by ERS- and caspase 12 was further promoted.

In summary, in the mouse model of post-infarction HF, the inhibition of MAPK signaling pathway suppressed cardiomyocyte apoptosis induced by MI or ERS. This pathway may be an eligible target for the prevention and treatment of post-infarction HF.

References

1. Wasilewski MA, Grisanti LA, Song J, Carter RL, Repas AA, Myers VD et al. Vasopressin Type 1A Receptor Deletion Enhances Cardiac Contractility, β-Adrenergic Receptor Sensitivity and Acute Cardiac Injury-induced Dysfunction. Clin Sci (Lond) 2016; pii: CS20160363.

2. Abtan J, Bhatt DL, Elbez Y, Sorbets E, Eagle K, Ikeda Y et al. Residual Ischemic Risk and Its Determinants in Patients with Previous Myocardial Infarction and Without Prior Stroke or TIA: Insights From the REACH Registry. Clin Cardiol 2016; doi: 10.1002/clc.22583.

3. Tse G, Yan BP, Chan YW, Tian XY, Huang Y. Reactive Oxygen Species, Endoplasmic Reticulum Stress and Mitochondrial Dysfunction: The Link with Cardiac Arrhythmogenesis. Front Physiol 2016; 7: 313.

4. Wei SG, Yu Y, Weiss RM, Felder RB. Endoplasmic reticulum stress increases brain MAPK signaling, inflammation and renin-angiotensin system activity and sympathetic nerve activity in heart failure. Am J Physiol Heart Circ Physiol 2016; 311 (4): H871–H880.

5. Liu Y, Qi SY, Ru LS, Ding C, Wang HJ, Li AY et al. Salubrinal improves cardiac function in rats with heart failure post myocardial infarction through reducing endoplasmic reticulum stress-associated apoptosis. Zhonghua Xin Xue Guan Bing Za Zhi 2016; 44 (6): 494–500.

6. Bozi LH, Jannig PR, Rolim N, Voltarelli VA, Dourado PM, Wisløff U et al. Aerobic exercise training rescues cardiac protein quality control and blunts endoplasmic reticulum stress in heart failure rats. J Cell Mol Med 2016; doi: 10.1111/jcmm.12894.

7. Mouw G. Activation of caspase 12, an endoplasmic reticulum resident caspase, after permanent focal ischemia in rat. Neuroreport 2003; 14: 183–186.

8. Zhang GG, Teng X, Liu Y, Cai Y, Zhou YB, Duan XH et al. Inhibition of endoplasm reticulum stress by ghrelin protects against ischemia/reperfusion injury in rat heart. Peptides 2009; 30 (6): 1109–1116.

9. Sreedhar R, Giridharan VV, Arumugam S, Karuppagounder V, Palaniyandi SS, Krishnamurthy P et al. Role of MAPK-mediated endoplasmic reticulum stress signaling in the heart during aging in senescence-accelerated prone mice. Biofactors 2016; 42 (4): 368–375.

10. Fu HY, Sanada S, Matsuzaki T, Liao Y, Okuda K, Yamato M et al. Chemical Endoplasmic Reticulum Chaperone Alleviates Doxorubicin-Induced Cardiac Dysfunction. Circ Res 2016; 118 (5): 798–809.

11. Gupta MK, Tahrir FG, Knezevic T, White MK, Gordon J, Cheung JY et al. GRP78 Interacting Partner Bag5 Responds to ER Stress and Protects Cardiomyocytes From ER Stress-Induced Apoptosis. J Cell Biochem 2016; 117 (8): 1813–1821.

12. Sreedhar R, Arumugam S, Thandavarayan RA, Giridharan VV, Karuppagounder V, Pitchaimani V et al. Depletion of cardiac 14-3-3η protein adversely influences pathologic cardiac remodeling during myocardial infarction after coronary artery ligation in mice. Int J Cardiol 2016; 202: 146–153.

13. Lou Y, Wang Z, Xu Y, Zhou P, Cao J, Li Y et al. Resveratrol prevents doxorubicin-induced cardiotoxicity in H9c2 cells through the inhibition of endoplasmic reticulum stress and the activation of the Sirt1 pathway. Int J Mol Med 2015; 36 (3): 873–880.

14. Cominacini L, Mozzini C, Garbin U, Pasini A, Stranieri C, Solani E et al. Endoplasmic reticulum stress and Nrf2 signaling in cardiovascular diseases. Free Radic Biol Med 2015; 88 (Pt B): 233–242.

15. Wei SG, Yu Y, Weiss RM, Felder RB. Inhibition of Brain Mitogen-Activated Protein Kinase Signaling Reduces Central Endoplasmic Reticulum Stress and Inflammation and Sympathetic Nerve Activity in Heart Failure Rats. Hypertension 2016; 67 (1): 229–236.

16. Liu Q, Tian J, Xu Y, Li C, Meng X, Fu F. Protective Effect of RA on Myocardial Infarction-Induced Cardiac Fibrosis via AT1R/p38 MAPK Pathway Signaling and Modulation of the ACE2/ACE Ratio. J Agric Food Chem 2016; 64: 6716–6722.

17. Vande Walle L, Jiménez Fernández D, Demon D, Van Laethem N, Van Hauwermeiren F, Van Gorp H et al. Does caspase 12 suppress inflammasome activation? Nature 2016; 534 (7605): E1–E4.

18. Song Y, Zhang C, Zhang J, Sun N, Huang K, Li H et al. An injectable silk sericin hydrogel promotes cardiac functional recovery after ischemic myocardial infarction. Acta Biomater 2016; 41: 210–223.

19. Cheng CY, Tang NY, Kao ST, Hsieh CL. Ferulic Acid Administered at Various Time Points Protects against Cerebral Infarction by Activating p38 MAPK/p90RSK/CREB/Bcl-2 Anti-Apoptotic Signaling in the Subacute Phase of Cerebral Ischemia-Reperfusion Injury in Rats. PLoS One 2016; 11 (5): e0155748.

20. Hosoi T, Ozawa K. Endoplasmic reticulum stress in disease: mechanisms and therapeutic opportunities. Clin Sci (Lond) 2010; 118: 19–29.

Received January 19, 2017.
Accepted February 20, 2017.